RSC Advances

ROYAL SOCIETY OF CHEMISTRY

www.rsc.org/advances

Magnetic chondroitin targeted nanoparticles for dual targeting of montelukast in prevention of in-stent restenosis

Jaleh Varshosaz[1,*], Shaghayegh Haghjooy Javanmard[2], Sahel Soghrati[1], Behshid Behdadfar[3]

[1]Department of Pharmaceutics, School of Pharmacy and Novel Drug Delivery Systems Research Centre, Isfahan University of Medical Sciences, Isfahan, Iran

[2]Physiology Research Center, Isfahan University of Medical sciences, Isfahan, Iran

[3]Department of Materials Engineering, Isfahan University of Technology, Isfahan, Iran

Running Head: *Magnetically targeted nanoparticles of montelukast*

*Corresponding author: Department of Pharmaceutics, Faculty of Pharmacy and Novel Drug Delivery Systems Research Centre, Isfahan University of Medical Sciences, Isfahan, PO Box 81745-359, Iran.

Email: varshosaz@pharm.mui.ac.ir

Abstract

Zinc substituted magnetic nanoparticles (MNPs) were prepared by hydrothermal reduction method and were encapsulated along with sodium montelukast within rosin gum nanoparticles (NPs) prepared by solvent evaporation method. The resulted NPs were targeted to endothelium cells by applying an outer layer of chondroitin sulfate on the surface of NPs. The characteristics of magnetic and rosin NPs were determined by Fourier transform infrared (FT-IR) spectroscopy, thermogravimetric analysis (TGA), transmission electron microscopy (TEM), and vibrating sample magnetometer (VSM). The heat capacity and crystalline state of citric acid (CA)-coated MNPs were analyzed by X-ray diffraction (XRD). The iron content in rosin NPs was determined by flame atomic absorption method. Bovine serum albumin (BSA) was used to test the protein binding of rosin NPs. Endothelial cell adhesion property of rosin NPs and their anti-inflammatory effect were studied on HUVEC cells by fluorescent microscopy and VCAM-1 Elisa analysis, respectively. TGA results confirmed the presence of CA and rosin on the surface of MNPs. The rosin NPs showed just 31% protein binding and the VSM analysis showed superparamagnetic property of in the coated NPs at room temperature. Targeted rosin NPs showed more adhesion to endothelial cells than non-targeted ones and montelukast loaded NPs were more efficient than free drug in suppression of VCAM-1 expression.

Key words: Montelukast, magnetic nanoparticles, rosin gum, chondroitin sulfate, in-stent restenosis

Introduction

In-stent restenosis is the serious complication of using stents for percutaneous coronary interventions. Inflammatory response, migration and proliferation of vascular smooth muscle cells from media to intima, arterial vessel remodeling and synthesis of extracellular matrix have an important role in development of neointimal hyperplasia.[1,2] One strategy for reduction and prevention of restenosis is using drug eluting stents (DESs). However, their use has many challenges like: 1) drug loading capacity is limited, 2) drug payload cannot be renewed, 3) release kinetics and drug dose cannot be adjusted, 4) drug resistance happens soon and 5) hyper sensitivity to the polymer or metal is usual.[3-5] Different techniques have been used to produce drug incorporated coatings on the stents such as immersion, chemical vapour deposition, ultrasonic atomization and plasma treatment.[6] However, the difficulty to control the thickness and composition as well as the complexity of the coating process hindered the successful use of these techniques to fabricate DESs for clinical applications. Nanoparticles have opened another promising pathway to resolve this problem. Compared to DESs, the nanoparticles approach is ideal due to the possibility of targeted delivery of drugs and reducing their systemic toxicity by using much lower doses.[6] Targeted delivery of nanoparticles is feasible by using a magnetic guidance. Magnetic targeting consists of a magnetic field source and biocompatible magnetically responsive drug carriers. This approach can reduce systemic drug exposure, side effects and improve the safety, efficacy of therapeutic agents by active guidance to the targeted area and selectivity of the therapy at significantly lower doses.[3,7] One study showed that the uniform field induced magnetization increased the retention of magnetic nanoparticles at target site and inhibited in-stent restenosis significantly with a relatively low dose of magnetic nanoparticles (MNPs)-encapsulating paclitaxel.[4] Furthermore, Vittorio Et al.[8] demonstrated that targeted delivery of

cathechin-dextran conjugate by magnetic nanoparticles can increase its intracellular concentration and anticancer efficacy. Particle properties should match with parenteral administration. The particle size should be below 1 µm preferably and nanoparticles of 100 to 200 nm are able to penetrate to inner layer of vessel wall but particles as large as 514 nm remains mainly at the luminal surface.[3,6]

Different studies showed that local delivery of anti-proliferation or anti-inflammatory agents decreases neointimal hyperplasia.[9,10] Anti-proliferative drugs have nonselective side effects. Despite of inhibition of vascular smooth muscle cells, they can affect endothelial cells repopulation and proliferation which leads to delayed vessel healing.[11-13] Anti-inflammatory drugs like cysteinyl leukoterian receptor antagonists are effective in prevention of restenosis. Leukoterians (LT) are pro-inflammatory agents that are generated from 5-lipoxygenase pathway and are produced by lukocyts and endothelial cells during vascular injury. There are 2 types of LTs: cysteinyl –LT (LTD4, LTE4, LTC4) and LTB4 that stimulate G-protein coupled cysteinyl–LT receptors (CysLT1, CysLT2). LTB receptors (LTB4 and LTD4) can cause intimal hyperplasia by stimulating proliferation and migration of vascular smooth muscle cells.[14,15] Montelukast, a Cys-LT receptor antagonist, inhibits the effect of LTD4 and suppresses the intimal hyperplasia.[15,16] Furthermore, studies revealed that levels of endothelial adhesion molecules like ICAM, VCAM-1, MCP-1, E-selectin and P-selectin are increased in patients with restenosis which increase the migration of leukocytes across the endothelium[17,18]. VCAM-1 has an important role in neointima formation in restenosis after arterial injury.[19] Other studies show that montelukast reduces the levels of MCP-1, VCAM-1, TNFα and IL-17 and has beneficial effect on progression of atheroscelerosis.[20,21]

To the best of our knowledge, no study has been reported on fabrication of targeted nanoparticles using LT receptor antagonists for prevention of restenosis. For this reason in the present study, dual targeted delivery of montelukast is provided by using MNPs and applying the outer layer of chondroitin sulfate by binding it to the nanoparticles carrying montelukast. It is reported that chondroitin is an endothelial adhesive agent, has low platelet adhesion properties and promotes wound healing too.[22,23] For this purpose, montelukast and MNPs were encapsulated within rosin gum and then coated with chondroitin sulfate.

Materials and methods

2.1. Materials

Ferric nitrate [$Fe(NO_3)_3.9H_2O$], ammonium hydroxide 25%, zinc chloride ($ZnCl_2$), dichloromethane and citric acid ($C_6H_8O_7.H_2O$), were purchased from Merck Chemical Company (Germany) with minimum purity of 99%. Fetal bovine serum (FBS) was from GIBCO Laboratories and montelukast was provided from MOrepen laboratory (New Delhi, India), chondroitine sulfate from Frabi Pharmaceutical Company (Iran), rosin gum and polyallylamine hydrochloride (MW 15000 Da) from Sigma Aldrich (USA). Deionized water freshly purged with nitrogen gas was used in all steps of the synthesis of magnetic nanoparticles and preparing all aqueous solutions. HUVEC cell line was supplied by Pasture institute (Iran). Dulbecco's phosphate buffered saline (PBS) and RPMI 1640 from BioIdea (Iran). Thiazolyl blue tetrazolium bromide (MTT) and 25% trypsin from Sigma (USA). DMEM medium from GIBCO Laboratories (Scotland), BMS232/BMS232TEN human VCAM-1 platinum ELISA kit was purchased from eBioscience (USA). Sterile DMSO was from Biosera Europe and TNF-α from eBioscience (USA).

2.2. Synthesis of magnetic nanoparticles

Three mmol of Fe^{3+} and 0.3 mmol Zn^{2+} salts were dissolved in 20 ml of distilled water and stirred for 10 min then a solution of 25% NH_4OH was added slowly to reach a pH medium of 9. Stirring continued strongly for another 10 min and a reddish brown slurry was formed. After that the slurry was centrifuged and washed three times with deionized distilled water to remove excess ions and reach a pH medium of 7. After that 6 mmol of citric acid was added to the mixture and it was stirred vigorously for 10 min and then transferred into a 500 ml volume teflon-lined autoclave at 180˚C for 20 h. The mixture was then cooled to room temperature and the precipitate was washed with acetone, mixing with 10 ml of deionized distilled water and sonicated for 10 min in an ultrasonic bath (Hawashin 505, Republic of Korea) to prepare the ferrofluids. The black suspensions were centrifuged for 10 min at 6000 rpm. The supernatant was the desired ferrofluids and the precipitate was discarded.

2.3. Preparation of rosin magnetic nanoparticles loaded with montelukast

Different amounts of rosin gum (10, 12.5 or 15 mg) and sodium montelukast (50, 75 or 100% with respect of rosin gum) were dissolved in 5 ml of dichloromethane, then citrated MNPs (850, 1000 or 1500 µg) were added to the solution and homogenized by high-performance dispersing instrument of ultra-homogenizer (IKA T 25 basic ULTRA-TURRAX®, Germany) at the power of 30 W for about 2 minutes until MNPs were dispersed in the solution. The mixture was added drop by drop to 25 ml of deionized water containing 1% of Tween 20 and homogenized at rate of 13500 rpm at room temperature to make an emulsion. Then the solvent was evaporated at room temperature by shaking the mixture on an orbital shaker (DAIKI Sciences, Republic of Korea) at rate of 187 rpm for 45 minutes.

Three different variables including rosin gum content (mg), MNPs ($ZnFe_3O_4$) content (µg), drug/gum ratio (%) were studied each in three levels (Table 1). To assess the effect of processing variables on the responses of particle size, zeta potential, drug loading efficiency (LE%), drug release after 20 days, and screening the most effective ones a Box-Benken design including 13 formulations (Table 2) was proposed by Design Expert Software (Version 7.2, USA). All experiments were done in triplicate.

Table 1. Description and trial levels of studied factors in preparation of magnetic nanoparticles loaded with montelukast

Studied variables	Levels		
	I	**II**	**II**
Gum rosin content (G) (mg)	10	12.5	15
Drug/gum (D/G) (%)	50	75	100
MNPs content (M) (µg)	850	1000	1500

Table 2. Different formulations of rosin nanoparticles loaded with MNPs and montelukast using Box-Benken design

Formulation code	Rosin Gum content (mg)	Drug/gum (%)	MNPs content (µg)
$G_{10}D_{75}M_{850}$	10	75	850
$G_{10}D_{50}M_{1000}$	10	50	1000
$G_{10}D_{75}M_{1500}$	10	75	1500
$G_{10}D_{100}M_{1000}$	10	100	1000
$G_{12.5}D_{100}M_{850}$	12.5	100	850
$G_{12.5}D_{100}M_{1500}$	12.5	100	1500
$G_{12.5}D_{75}M_{1000}$	12.5	75	1000
$G_{12.5}D_{50}M_{1500}$	12.5	50	1500
$G_{12.5}D_{50}M_{850}$	12.5	50	1000
$G_{15}D_{75}M_{850}$	15	75	850
$G_{15}D_{75}M_{1500}$	15	75	1500
$G_{15}D_{100}M_{1000}$	15	100	1000
$G_{15}D_{50}M_{1000}$	15	50	1000

2.4. Preparation of chondroitin targeted nanoparticles

Solutions of 4 mg poly(allylamine) hydrochloride in 10 ml of deionized water and 10 mg chondroitin sulfate in 25 ml of deionized water were prepared separately. Then 0.4 ml of chondroitin sulfate solution was added drop by drop to 10 ml solution of poly(allylamine) while stirred at 400 rpm to make a layer by layer conjugate of chondroitin sulfate to poly(allylamine) and produce chondroitin sulfate/poly(allylamine) hydrochloride conjugate. One ml of conjugated polymer solution (containing 15.68 µg of chondroitin sulfate) was added to the previously prepared NPs by slow shaking on an orbital shaker at rate of 160 rpm at room temperature to let the conjugate to attach the particles by electrostatic bonds. Figure 1 shows the schematic structure of the prepared nanoparticles.

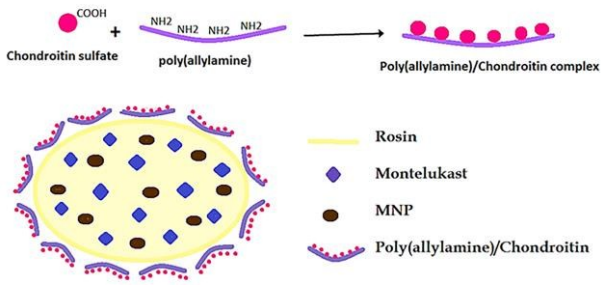

Figure 1. Schematic representation of the structure of rosin nanoparticles loaded with magnetic nanoparticles (MNP) and montelukast

2.5. Particle size and zeta potential measurement of rosin nanoparticles loaded with MNPs

The mean particle size and zeta potential of MNPs were determined using Zetasizer (Zetasizer-ZEN 3600 Malvern Instrument Ltd., Worcestershire, UK). For these measurements samples with concentration of 1 mg/ml of NPs in deionized distilled water were used. The hydrodynamic size was measured at pH 7 and the intensity data were analyzed to obtain the Z-average size. Zeta potential of dispersions was measured at different pH values between 2 and 12. An average diameter and distribution of particle size and zeta potential was reported from runs of 3 and 2,

respectively. Furthermore, the mean particle size and zeta potential of rosin nanoparticles encapsulating MNPs and drug was measured by the same device to measure mean particle size and zeta potential of the nanoparticles before and after coating with chondroitin sulfate/poly(allylamine) hydrochloride conjugate by 1:1 dilution of sample with deionized water at room temperature.

2.6. Determination of montelukast loaded in rosin magnetic nanoparticles

Drug loading efficiency (LE%) was determined by measuring the concentration of un-encapsulated or free drug in aqueous medium. For this purpose 400 μl of the drug loaded nanoparticles was centrifuged (Micro-centrifuge Sigma 30k, UK) at 10000 rpm for 5 min in micro-centrifuging filter tubes (Amicon Ultra, Ireland) with a 10 kDa molecular weight cutoff, and the concentration of free drug in the aqueous medium was measured by a UV-visible spectrophotometer (UV-mini 1240, Shimadzu, Kyoto, Japan) at λ_{max}=277.9 nm. Blank nanoparticles were used as control. The amount of entrapped drug was determined through the difference between the total and the free drug. Loading efficiency (LE%) was calculated by the following equation:

$$\text{Drug loading efficiency \%} = \frac{Total\ drug - free\ drug}{Total\ drug} \times 100 \qquad \text{eq. 1}$$

2.7. Drug release studies

Two ml of each nanoparticle dispersion was transferred to a dialysis bag (Mw cutoff 12000, Membra-Cel, Viskase, USA), and the bag was placed in phosphate buffer solution (pH 7.4) containing 1% Tween 20 while shaken on an orbital shaker bath at rate of 120 rpm and at 37°C. 600 μl samples were taken and montelukast absorbance in each sample was measured at λ_{max}=284.5 nm at specific time intervals. Afterwards the samples were transferred back to the release medium.

2.8. Determination of iron content in rosin nanoparticles

The iron content in rosin nanoparticles was determined by flame atomic absorption spectrophotometer (PERKIN-ELMER 2380, USA). For this purpose 2 ml of nanoparticle suspension was examined at wavelength of 248.3 nm based on a previously established calibration curve. Fe_3O_4 loading efficiency was calculated as the ratio of iron oxide in 100 ml of its dispersion.

2.9. Physical characterization of MNPs and rosin nanoparticles loaded with MNPs and drug

For the physical characterization of citric acid coated MNPs the Fourier transform infrared (FT-IR) spectra, X-ray diffraction (XRD) and thermogravimetric analysis (TGA) were performed. Besides, the physical characterization of optimal formulation of rosin nanoparticles loaded with MNPs was analyzed by FT-IR spectroscopy. The citric acid, rosin and chondroitin/poly(allylamine) conjugate content of the nanoparticles were determined by thermogravimetric analysis (TGA). The FT-IR of particles was recorded employing a FT-IR Spectroscope (JASCO, FT/IR-6300, Japan). Data was acquired in range of 400–4000 cm^{-1}. X-ray diffraction (XRD) patterns of MNPs were recorded employing an X-ray diffractometer (Bruker-D8 ADVANCED, USA) using a Cu anode at λ=1.5406Å. The samples were mounted on double sided silicone tape and measurements were performed at 2θ from 20 to 70˚. Scherrer's formula, $d=(\frac{0.9\lambda}{\beta cos\theta})$, was used to estimate the mean crystallite size. Where λ is the X-ray wavelength and equal 1.5406A˚, β is the line broadening at half the maximum intensity equal to 0.018° and θ is the Bragg angle. Thermo-analytical technique of rosin nanoparticles and MNPs was accomplished on a simultaneous Thermal Analysis device (STA) (LINSEISL81/1750-PLATINUM, Germany) from 25˚-900˚C at a heating ramp of 10˚C/min, under argon gas flow.

2.10. Particles Morphology

The morphology of citric acid coated MNPs and also the optimal formulation of rosin nanoparticles loaded with MNPs were evaluated by transmission electron microscope (Zeiss, EM10C, Germany). For TEM the samples were prepared by placing a droplet of the suspension on to a 300 mesh carbon coated copper grid and allowed to be dried in air naturally. Finally, micrographs were taken with different levels of magnification with an accelerating voltage of 80 kV.

2.11. Magnetic properties of rosin nanoparticles

Magnetic properties of the prepared MNPs and the rosin nanoparticles loaded with MNPs were measured by a vibrating sample magnetometer (VSM) (AGFM/VSM 3886 Kashan, Iran) at room temperature in a magnetic field strength of 1 Tesla.

2.12. Protein binding measurements

To determine the protein binding interaction with rosin nanoparticles, 1 ml of BSA solution (330 µg/ml) was added to 1 ml of the optimal formulation of rosin nanoparticles (1 mg/ml) loaded with MNPs and the mixture was shaken for 1 h at 150 rpm at 37˚C. Then the mixture was filtered by a Millipore filter with porosity of 50 nm and the UV absorbance of the resulting solution was evaluated by the UV-visible spectrophotometer at λ_{max}=277.5 nm. Finally the results were compared with the total UV absorption of the blank (nanoparticles without BSA) at the same wave length.

2.13. *In vitro* evaluation of endothelial cells adhesion

HUVEC cells were seeded at 3×10^4cells/ml on 6-well tissue culture dish and incubated for 24 h within humidified 5% CO_2 incubator set at 37˚C to allow them to attach. Chondroitin coated and non-coated nanoparticles loaded with pyrene (as a fluorescent probe) were added to different wells

and incubated for 2 h within humidified 5% CO_2 incubator set at 37˚C. Then, the wells were washed 2 times with phosphate buffer solution (PBS) to remove non-attached NPs before imaging on light and fluorescent microscope (CETI Magnum-T, medline UK).

2.14. Cell viability assay

The cell viability of HUVEC cells was measured by MTT assay to evaluate the cytotoxicity of nanoparticles. After cells were seeded at 10^4cells/ml on 96-well plate, each row was treated with 20 µl of chondroitin coated NPs without drug at the same concentration used for drug loaded NPs (10^{-9}, 10^{-7} and 10^{-5} M) and 20 µl of culture medium (as negative control). Afterward, the plate was incubated for 48 h and after discarding the medium, 100 µl of RPMI were added. Then 10 µl of MTT solution (5 mg/ml) was added to each well. Following 4 h of incubation, the cell medium was removed and 70 µl of DMSO was added to each well to solubilize Formazan crystals. Finally, the plate was subjected to absorbance read at 570 nm with a microplate reader. All experiments were performed in triplicate. Cell viability for each sample was calculated using equation (2):

$$Cell\ survival\% = \frac{(Mean\ of\ each\ group - mean\ of\ blank)}{(\text{mean of negative control} - \text{mean of blank})} \times 100 \qquad \text{eq.2}$$

2.15. *In vitro* evaluation of anti-inflammatory effect of montelukast loaded NPs on endothelial cells

HUVEC cells were seeded at 10^4cells/ml on 96-well tissue culture dish and incubated for 24 h within humidified 5% CO_2 incubator set at 37˚C to allow them to attach. The cells were then treated with free montelukast, rosin nanoparticles loaded with montelukast, and blank chondroitin coated rosin NPs at concentrations of (10^{-5}, 10^{-7}, 10^{-9} M) for 48 h. Then the cells were stimulated by TNFα (10 ng/ml) for 6 h and the supernatant was aspirated for ELISA analysis of VCAM-1.

2.16. Statistical analysis

The effects of the studied variables on the *in vitro* responses were analyzed by the Design Expert Software (Version 7.2, USA) to obtain independently the main effects of these factors, followed by the analysis of variance (ANOVA) to determine which factors were statistically significant. The optimum conditions were determined by the optimization method to yield a heightened performance. Values were processed using Microsoft Excel 2013 and SPSS Statistics (ver. 22, USA) using analysis of variance (ANOVA) followed by the post hoc test of LSD and the level of significance was set at $P < 0.05$.

3. Results and discussion

3.1. Synthesis of magnetic nanoparticles

Among different methods for synthesizing Zn substituted magnetic nanoparticles[24-28], hydrothermal reduction method was chosen because of disadvantages of other methods like instability of NPs in aqueous medium at pH 7, requiring high temperature (>600°C), size limitation and wide particle size distribution. However, in hydrothermal reduction method the reaction temperature is lower (<200°C), produces particles with controlled size and water dispersible MNPs. Hence, this method was used in presence of safe and cheap reducing agent, citric acid (CA), to produce aqueous ferrofluids which can be encapsulated within rosin nanoparticles.

3.2. Characterization of CA-coated MNPs and rosin NPs encapsulating MNPs and montelukast

3.2.1. Particle size and zeta potential

Particle size of MNPs was obtained in aqueous medium (pH 7) by using DLS method. The mean Z-average was 92.1 nm with the polydispersity index (PDI) of 0.144 which indicates that

ferrofluids are mono dispersed and have low diversity of particle size. Zeta potential was measured at different pH values between 2 and 12. MNPs had negative surface potential around -25 mV at pH 7 which confirms the presence of CA on the surface of NPs. Morphology and particle size of NPs can be controlled by adjusting pressure, temperature and time. Recrystallization of spinel phase starts to 90°C and continues to 200°C.[29,30] In the present study, we used 180°C for 20 hours to obtain mono disperse particles with desirable size and crystal shape. MNPs were coated by CA to avoid agglomeration, oxidation and limit the size distribution.[31,32] The resulted CA coated MNPs and montelukast sodium were encapsulated within rosin gum and coated by polyallylamine/chondroitin conjugate.

In preparing rosin gum NPs changing the levels of rosin content, drug/rosin ratio (D/G) and MNPs content had no significant effect on particle size ($P>0.05$). However, rosin content and D/R ratio had significant impact on zeta potential ($P<0.05$). Increase in rosin content led to raising in absolute value of zeta potential due to the negative charge of rosin gum in water. Therefore, the more rosin content, the more negative zeta potential of NPs. Raise in D/G ratio made the zeta potential more negative due to the negative charge of montelukast.

Polyallylamine solution had a zeta potential of 30 mV and after adding 0.4 ml of chondroitin sulfate solution it decreased to 22.5 mV which indicated the formation of polyallylamine/chondroitin complex. Then as Table 3 shows mixing the rosin NPs with this complex increased their zeta potential which confirmed the coating of NPs with the polyallylamine/chondroitin complex.

To show the effect of studied parameters on particle size and zeta potential of NPs the full second-order polynomial equation (quadratic model) was generated by Design Expert Software.

$$Y=\beta_{\circ} + \beta_1 G + \beta_2 (D/G) + \beta_3 M + \beta_{11} G^2 + \beta_{22} (D/G)^2 + \beta_{33} M^2 + \beta_{12} G(D/G) + \beta_{13} GM + \beta_{23} (D/G)M \quad \text{eq. 3}$$

Where Y is predicted response(s), $\beta_{\circ}$ is an intercept, β_1, β_2, and β_3 are linear coefficients, β_{11}, β_{22}, and β_{33} are squared coefficients and quadratic term, β_{12} , β_{13}, and β_{23} are interaction coefficients, and *G*, *D/B*, and *M* are independent variables defined in Table 1 which are selected based on the results from study. In the following equations the positive sign means synergism effect of the variables on the response but the negative sign indicates a lowering effect on it.

$$\textit{Particle size} = 152.10 + 11.63G + 5.33(D/G) - 16.75M - 14.13G(D/G) + 28.23GM - 2.63(D/G)M - 30.11G^2 - 18.01(D/G)^2 + 20.63M^2 \quad \text{eq. 4}$$

$$\textit{Zeta potential} = -12.5 - 14.25G - 8.56(D/G) - 1.29M + 0.13G(D/G) - 0.025GM - 0.2(D/G)M + 7.2G^2 + 3.28(D/G)^2 + 3.18M^2 \quad \text{eq. 5}$$

Table 3. Particle size, zeta potential, drug loading efficiency and drug release of different rosin gum nanoparticles encapsulating MNPs and montelukast coated by polyallylamine/chondroitin complex

Formulation code	Particle size (nm) ± SD	Zeta potential before coating (mV)	Zeta potential after coating (mV)	Loading efficiency (%) ± SD	Release at 20 days (%)± SD
$G_{10}D_{75}M_{850}$	194.3±6.9	-10.6	15.7	99.8±0.0	34.4±7.1
$G_{10}D_{50}M_{1000}$	43.6±1.7	-4.3	17.3	94.9±0.9	55.2±5.5
$G_{10}D_{75}M_{1500}$	88.0±2.0	-8.3	12.1	99.6±0.0	59.0±9.7
$G_{10}D_{100}M_{1000}$	120.9±1.2	-22.8	3.6	99.7±0.5	40.9±3.6
$G_{12.5}D_{100}M_{850}$	152.1±1.8	-25.0	-15.5	99.8±0.2	56.8±5.7
$G_{12.5}D_{100}M_{1500}$	129.7±2.4	-26.5	-17.4	99.4±0.6	49.6±4.1
$G_{12.5}D_{75}M_{1000}$	152.1±0.4	-24.0	-12.5	99.7±0.4	45.3±1.9
$G_{12.5}D_{50}M_{1500}$	162.7±7.5	-17.7	3.8	97.4±0.1	43.8±9.0
$G_{12.5}D_{50}M_{850}$	174.6±7.1	-19.7	4.9	99.7±0.5	50.1±7.8
$G_{15}D_{75}M_{850}$	140.9±0.9	-28.3	-16.3	99.5±0.0	50.1±3.2
$G_{15}D_{75}M_{1500}$	147.5±0.7	-27.9	-20.0	99.6±0.6	27.7±2.4
$G_{15}D_{100}M_{1000}$	136.1±1.4	-28.3	-21.1	99.7±0.2	34.8±1.1
$G_{15}D_{50}M_{1000}$	115.3±2.5	-25.1	-7.9	97.5±0.1	25.0±5.1

3.2.2. Determination of montelukast loaded in the rosin nanoparticles

None of the studied variables had significant effect ($p>0.05$) on montelukast loading efficiency. A 2FI model showed the effect of studied variables on drug LE%:

$$LE\% = 0.29G + 1.14(D/G) - 0.35M - 0.065G(D/G) + 0.075(D/G)M - 0.6G^2 - 1.15(D/G)^2 + 0.521M^2 \quad \text{eq. 6}$$

3.2.3. *In vitro* release of montelukast from rosin nanoparticles loaded with MNPs

Release profile of montelukast during 20 days is illustrated in Figure 2 for the studied formulations. This figure indicates that all formulations have slow release pattern with zero order kinetic in phosphate buffer solution (PBS) (pH 7.4) containing 1% of Tween 20.

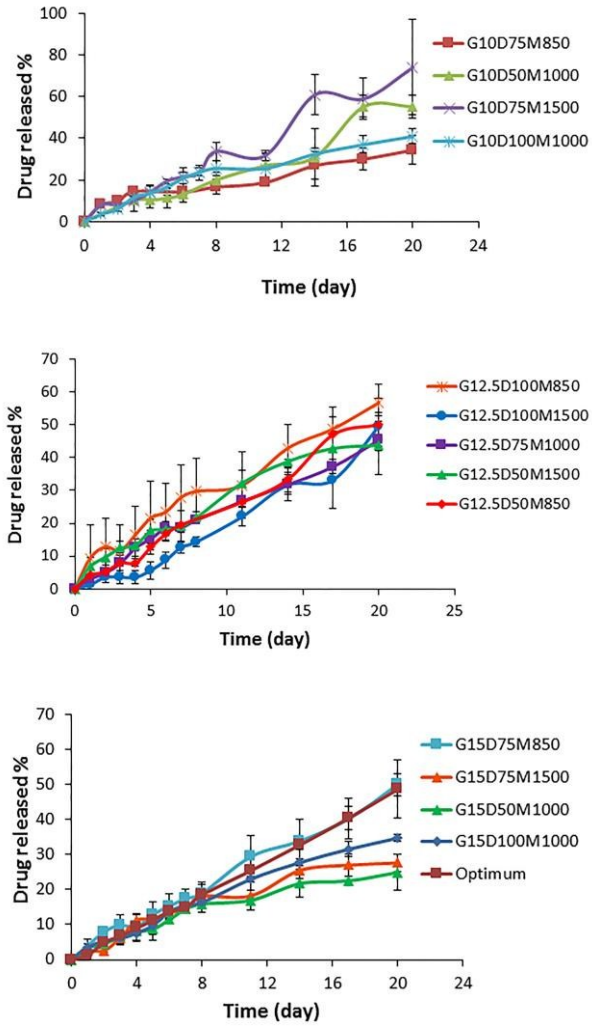

Figure 2. *In vitro* release profile of montelukast from different studied formulations. In all formulations G stands for the rosin gum content, D for the ratio of drug/polymer and M for the MNPs content. Each point represents as mean±SD, (n = 3)

Rosin content was the most important variable that had significant effect on release profile ($P<0.05$). Increase in polymer content decreased the release rate (Figure 2). Table 3 also indicates that changing in rosin content from 10 to 12.5 mg didn't show a great decrease in drug release after 20 days but increasing in its content from 12.5 to 15 mg caused a considerable decrease in it ($P<0.05$). Lee et al.[33] prepared rosin nanoparticles for controlled delivery of hydrocortisone. They observed that as the rosin content of NPs increased, the drug release decreased gradually and concluded that rosin was a suitable carrier for sustained release of the drug. In addition, Zhuet et al.[34]demonstrated that increasing in chitosan content in preparation of chitosan-coated magnetic NPs carrying of 5-fluorouracil the polymer content could slow down the release of the drug by forming a thicker wall. A quadratic model was proposed by the software for estimation of the drug release percent after 20 days:

$$Drug\ release\ \% = 45.33 - 6.49G + 1.01(D/G) - 1.43M + 6.02G(D/G) - 11.75GM - 0.22(D/G)M - 6.82G^2 + 0.48(D/G)^2 + 4.28M^2 \quad \text{eq. 7}$$

3.2.4. Physical characterization of magnetic and rosin NPs

To confirm the presence of citrate ion on the surface of $ZnFe_3O_4$ nanoparticles, FT-IR analysis was done (Figure 3a). The peak at 3396.99 cm^{-1} shows the structural OH group. The strong peak at 1690-1760 cm^{-1} shows the symmetric stretching vibration of C=O of carboxylic acid group of CA. This peak has shifted to 1613 cm^{-1} in the magnetic nanoparticles coated with CA which indicates the binding of citric acid radicals to the surface of MNPs. Sharp peak in 572.75 cm^{-1} is due to Fe-O bonds and shows the magnetic phase.

FTIR spectrum of polyallylamine /chondroitin coated rosin gum nanoparticles which were loaded with MNPs in shown in Figure 3b. The sharp peak at 571 cm^{-1} relates to magnetic phase. The peak seen at 1694.16 cm^{-1} belongs to C=O acidic group of CA, rosin gum and chondroitin sulfate. The peaks between 1350-1000 cm^{-1} relate to C-N stretching band of amine group of polyallylamine and that seen in 1150 cm^{-1} is probably related to the C-O group of carboxylic acid of CA, rosin, and chondroitin sulfate. The peak in 1650-1450 cm^{-1} relates to aromatics and a medium peak at 1462.74 cm^{-1} indicates the aromatic ring of rosin. A weak peak at 1644 cm^{-1} confirms the C=C bond and at 3425.92 cm^{-1} shows the NH_2 group of polyallylamine and N-H of amide group of chondroitin sulfate. Two asymmetric and symmetric absorption bands of S=O at 1385.6 and 1150.33 cm^{-1}, respectively confirm the sulfate group of chondroitin sulfate.

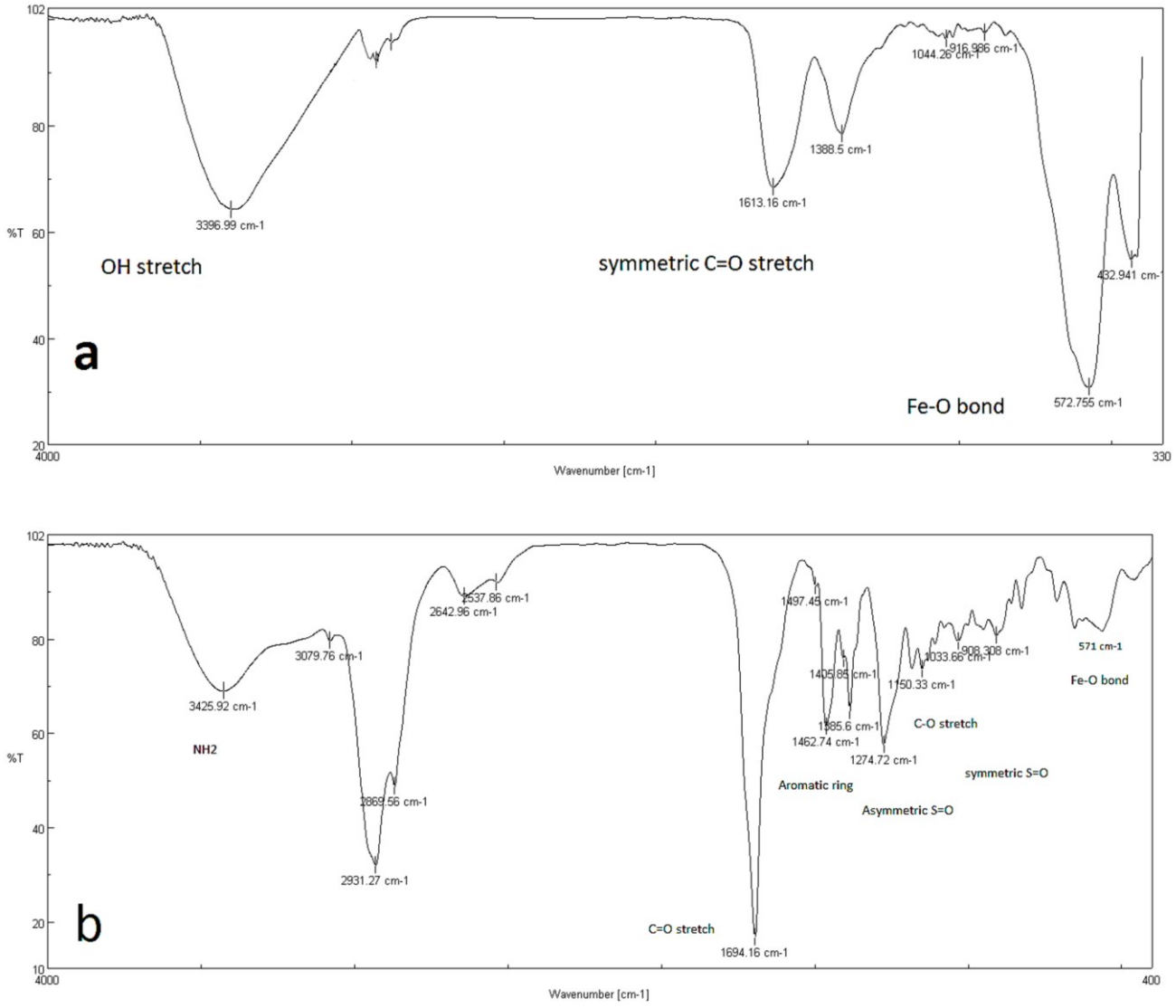

Figure 3. FTIR spectra of a) citrate coated magnetite nanoparticles and b) rosin nanoparticles encapsulating MNPs and coated with polyallylamine/chondroitin sulfate

Figure 4 shows XRD pattern of the CA coated MNPs. The intense peaks seen at 2θ of 30.1, 35.5, 43.2, 53.4, 57.5, 62.7 relate to spinel structure as single phase Fe_3O_4. Calculated mean crystallite size by Scherrer's equation is: $Particle \quad size = \frac{0.9\lambda}{\beta \cos \theta}$ where λ is the X-ray wavelength and equal 1.5406A°, β is the line broadening at half the maximum intensity equal to 0.018° and θ is the Bragg angle equal to 35.5/2=17.75. This makes the crystal size as much as 8.2 nm.

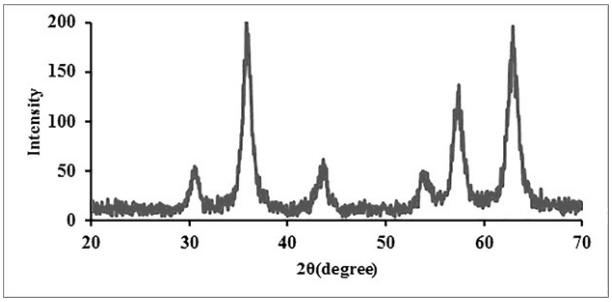

Figure 4. XRD pattern of the CA coated MNPs

To confirm the presence of CA and rosin on the surface of MNPs thermogaravimetry analysis (TGA) was done (Figure 5). CA-coated MNPs had a weight loss around 2.75% at 282˚C which belonged to CA while, rosin nanoparticles which encapsulated MNPs showed 0.2% weight loss at 282˚C that is related to CA and 70.27% weight loss at 300˚C relating to rosin gum removal due to its burning. The results showed totally 87.06% weight loss that shows iron content of these nanoparticles was approximately 12.94%.

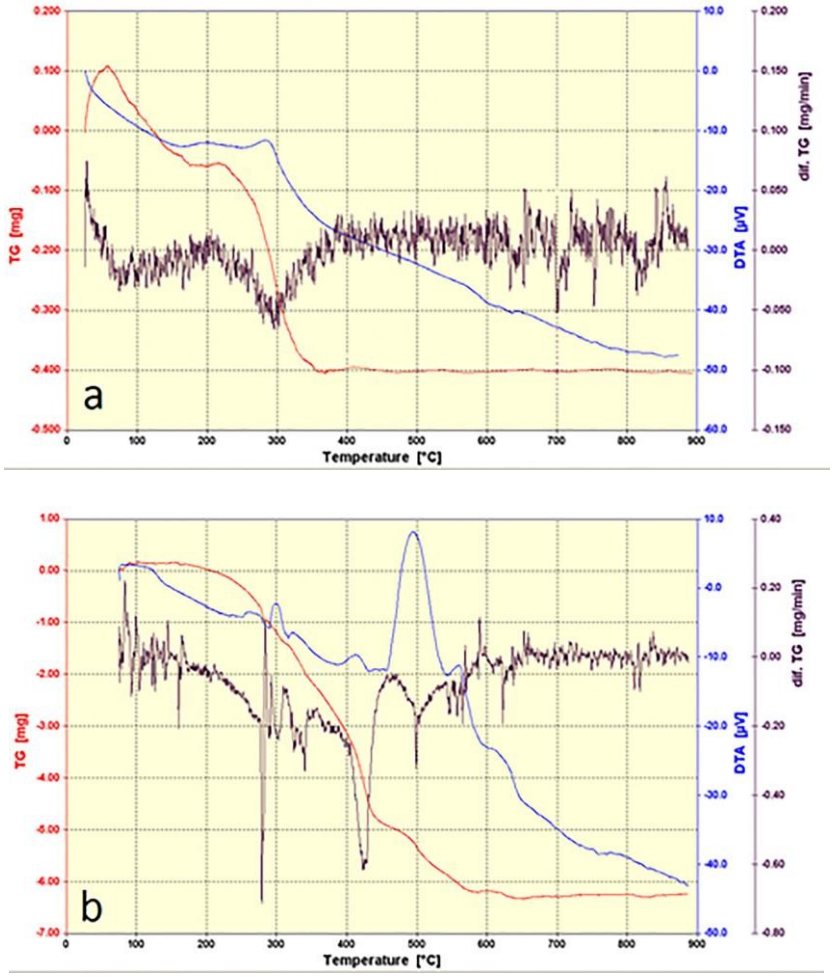

Figure 5. TGA of a) CA coated MNPs and b) rosin nanoparticles encapsulating MNPs

3.2.4. Morphology of nanoparticles

TEM images of MNPs are shown in Figure 6a. Uniformity in shape and particle size can be seen in the micrographs. According to the scale bar, the particle size of these NPs is 8.4 nm which is in agreement with Scherrer's result discussed before. TEM images of rosin NPs encapsulating MNPs and coated with polyallylamine/chondroitin sulfate conjugate is shown in Figure 6b. Images show the size and shape uniformity of these NPs which is between 10.8-11.6 nm.

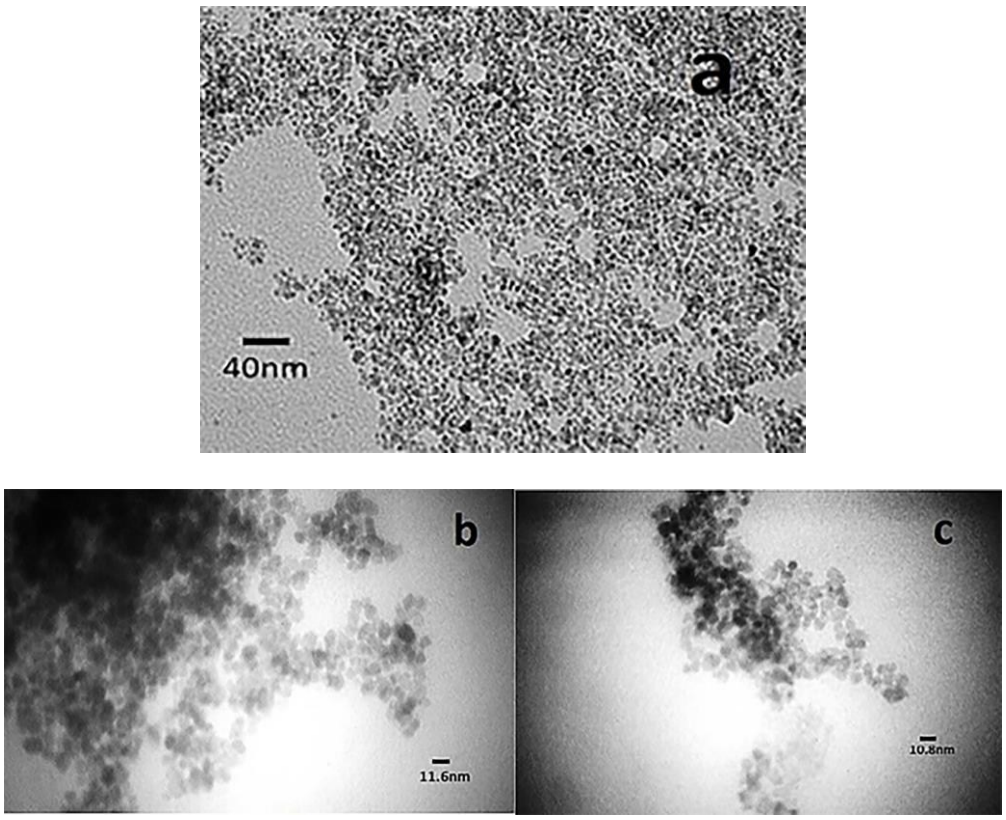

Figure 6. TEM images of a) CA coated MNPs and b, c) rosin NPs encapsulating MNPs and coated with polyallylamine/chondroitin sulfate conjugate

3.2.5. Magnetic properties of NPs

The superparamagnetic property of CA-coated MNPs and rosin NPs loaded with MNPs is shown in Figure 7. The VSM analysis was done at room temperature and the saturation magnetization (σ_s) was determined to be 48.16 and 3.46 emu/g for CA-coated MNPs and rosin NPs loaded with MNPs, respectively. The reduction in saturation magnetization compare to CA-coated MNPs is due to low magnetic loading and thick wall of rosin gum around MNPs.

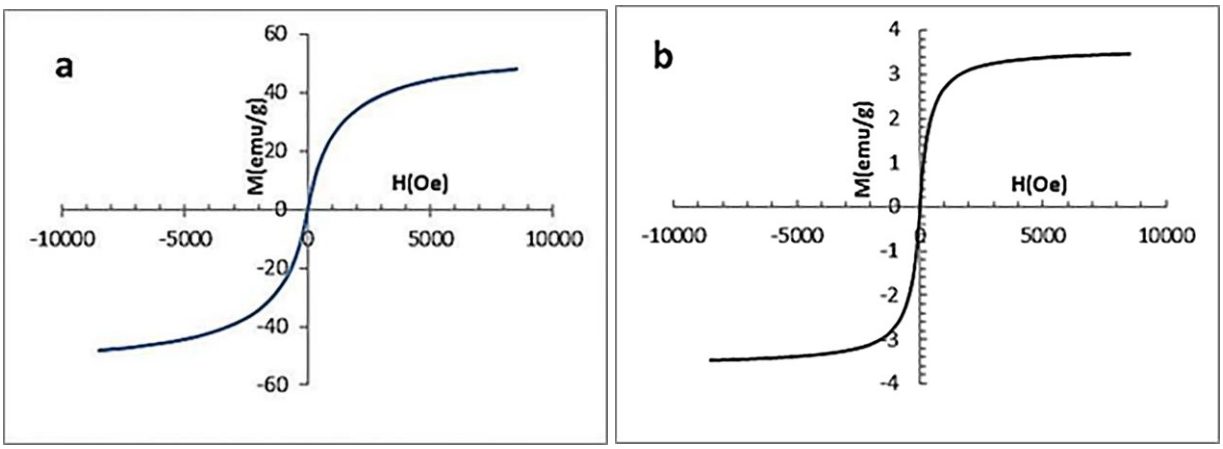

Figure 7. VSM curves of a) CA-coated MNPs and b) rosin NPs encapsulating MNPs

3.2.6. Determination of iron content in rosin NPs

The atomic absorption analysis confirmed the entrapment of 10.83% of superparamagnetic $ZnFe_3O_4$ NPs into rosin NPs which confirmed the results of TGA analysis (Figure 5b).

3.3. Optimization

Computer optimization process by Design Expert Software (Version 7.2, US) and a desirability function determined the effect of the levels of independent variables on the responses. Optimization for response factors included: minimum particle size while, maximum absolute value of zeta potential, the loading efficiency and drug release at 20 days. Solution provided by the software with the greatest desirability was chosen as the optimum condition and after executing the experiment based on the suggested values for the independent factors of rosin gum and MNPs content and drug/gum ratio, the real responses were compared with the predicted ones and error percent was calculated to evaluate the predictive ability of the models. The optimum formulation suggested by the software included the rosin gum content of 10.7 mg, drug/rosin ratio of 62.23% and MNPs content of 1486 µg. The actual and predicted values of responses are shown in Table 4. The error percent in predicting all responses by the software was below 20% which shows that the actual responses are in close accordance with the predicted values and the potential application

of Box-Behnken model for estimation of physicochemical properties of rosin nanoparticles loaded with MNPs.

Table 4. Comparison of the Design Expert predicted and actual values of responses studied in rosin nanoparticles encapsulating MNPs and montelukast and coated with polyallylamine/chondroitin

Responses	Particle size (nm)	Zeta potential (mV)	Loading efficiency (%)	Release at 20 days (%)
Predicted	67.4	5	97.9	59.1
Actual	63.8±2.3	5.53	99.1±0.2	48.8±8.4
Error %	3.6	-10.6	-1	17

3.4. Protein binding of NPs

Any protein absorption by the surface of nanoparticles in serum can change the pharmacokinetic fate of nanoparticles before their reaching the intended target. The protein binding test of rosin nanoparticles encapsulating MNPs and montelukast and coated by polyallylamine/chondroitin revealed that 33.56% of albumin is bonded to the nanoparticles. In a study on using magnetic polyvinyl caprolactam–polyvinyl acetate–polyethylene glycol micelles for docetaxel delivery in breast cancer the protein binding was reported as much as 10% by the micelles[35]. Varshosaz et al.[36] also used nano magnetic micelles conjugated by luteinizing hormone-releasing hormone (LHRH) peptide for dual targeting of doxorubicin in breast cancer and reported protein binding of 31% for their nanomicelles. The reported range of protein binding by different carrier systems for magnetic nanoparticles lies between 10-35%.

3.5. *In vitro* evaluation of adhesion of nanoparticles to endothelium cells

To compare the effect of the presence of chondroitin as the targeting agent on the surface of rosin NPs in their adhesion to the endothelial cells images were taken by fluorescent microscope shown in Figure 8. The NPs were loaded with pyrene (as a fluorescent probe). Figures 8a and b confirm

the dispersion of equal number of HUVEC cells in the 2 studied groups; one treated with targeted and the other with non-targeted rosin NPs. Comparing images of 8c and 8d indicate more fluorescence accumulation in the cells treated with the chondroitin sulfate coated NPs than non-coated ones. The results agree well with Thalla et al.[22] and Heng et al.[23] studies who showed that chondroitin had endothelium cell adhesion properties and might be used as an appropriate targeting agent to the endothelial tissues.

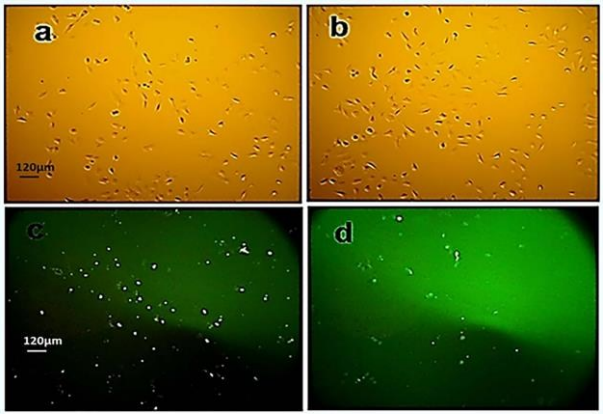

Figure 8. The visible light (upper row) and fluroscent microscopy (lower row) images of HUVEC cells treated with (a, c) chondroitin targeted NPs and (b, d) non-targeted rosin NPs (magneficaiton, 10×)

3.6. Cell viability assay

The results of the MTT assay are shown in Figure 9. Analyzing the results of this test by SPSS software (version 22, US) showed that there is no significant difference between the treated groups and the negative group ($p>0.05$). In other words the NPs showed no cytotoxicity on the HUVEC cells.

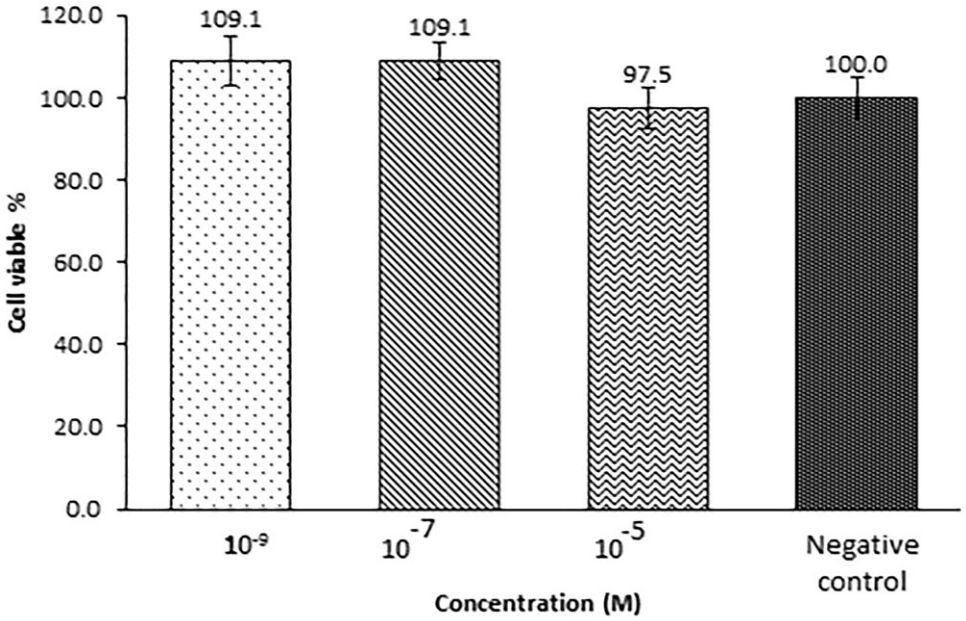

Figure 9. Viability of HUVEC cells after treatment with different concentrations of targeted NPs compared to negative control by MTT assay

3.7. *In vitro* evaluation of anti-inflammatory effect of motelukast on endothelium cells

After the HUVEC cells were stimulated by TNFα (10 ng/ml) for 6 h the levels of soluble VCAM-1 in culture supernatants were measured as shown in Figure 10. Analyzing the data by SPSS software (version 22, US) showed that the level of VCAM-1 was significantly lower ($P<0.05$) in cells treated with montelukast in comparison with non-treated cells which were stimulated by TNF-α. Expression of VCAM-1 in treated cells with montelukast loaded NPs was significantly lower than free montelukast ($P<0.05$) which indicated that rosin NPs encapsulating MNPs and montelukast were more efficient than free drug in suppression of VCAM-1 expression. This is possibly due to the presence of chondroitin on the surface of the NPs which can attach to the hyaluronan endocytosis receptors which are overexpressed on the surface of endothelial cells.[37,38] Concentration of 10^{-5} and 10^{-7} in free and loaded drug NPs were more efficient than 10^{-9} M ($P<0.05$) but there was no significant difference between 10^{-5} and 10^{-7} M in suppression of VCAM-

1 expression. Pigott et al.[39] found that soluble forms of E-selectin, ICAM-1 and VCAM-1 are present in the supernatants of cytokine activated endothelial cells and Hadi et al. [20] studies also showed that montelukast can reduce the inflammatory marker of VCAM-1.

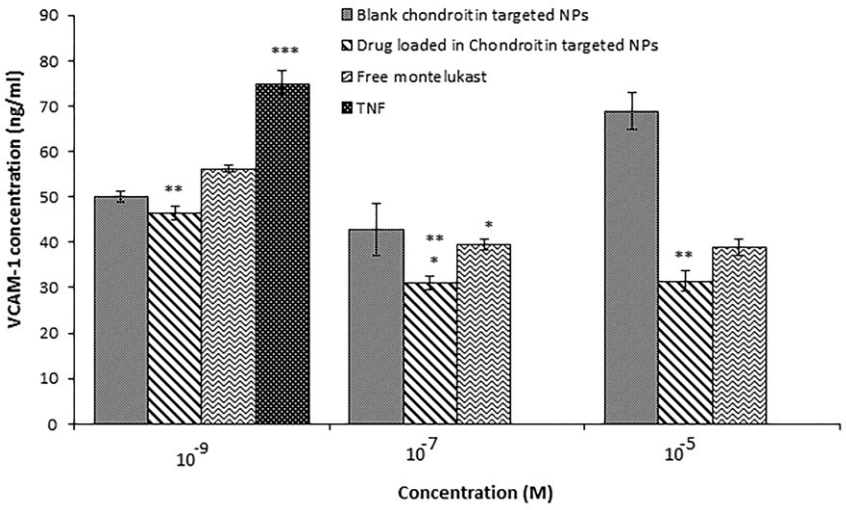

Figure 10. Anti-inflammatory effect of different concentrations of free montelukast, blank targeted and montelukast loaded in chondroitin targeted rosin NPs on suppressing the expression of VCAM-1 on HUVEC cells stimulated by 10 ng/ml TNFα for 6 hours. (* shows significant difference with the same group at lower concentration ($P<0.05$). ** shows significant difference with free drug at the same concentration ($P<0.05$). *** shows significant difference with other groups ($P<0.05$).)

Conclusion

Rosin nanoparticles loaded with montelukast and MNPs were prepared to prevent in-stent restenosis. For this purpose rosin gum was used to encapsulate CA- coated MNPs and drug due to its capability to sustain the drug release. The nanoparticles were targeted to endothelial cells by coating them with chondroitin sulfate. CA-coated MNPs were synthesized by hydrothermal reduction method. The best formulation of rosin nanoparticles prepared by solvent evaporation

method included the rosin gum content of 10.7 mg, drug/rosin ratio of 62.23% and MNPs content of 816.75 µg. Targeting the nanoparticles with chondroitin sulfate showed more adhesion to HUVEC cells than non-targeted ones which indicates the capability of using chondroitin sulfate as a targeting agent for endothelial cells. The expression of VCAM-1 in TNF-α stimulated cells was significantly suppressed in the cells treated with montelukast loaded nanoparticle at concentration of 10^{-7} M of the drug. These findings show the potential of targeted rosin nanoparticles loaded with montelukast in suppression of inflammatory path way to prevent the restenosis by dual targeting using a magnetic field guide and chondroitin sulfate coated layer. The results should be checked *in vivo* to confirm the promising results obtained from the cell culture tests.

Acknowledgements

The authors appreciate supports of this project by Isfahan University of Medical Sciences.

References

1. G. M. Lanza, X. Yu, P. M. Winter, D. R. Abendschein, K. K. Karukstis, M. J. Scott, L. K. Chinen, R. W. Fuhrhop, D. E. Scherrer, S. A. Wickline, *Circulation*, 2002, **106**, 2842 2847.
2. Y. Huang, K. Salu, X. Liu, S. Li, L. Wang, E. Verbeken, J. Bosmans, I. D. Scheerder, *Heart*, 2004, **90**, 195 199.
3. M. Chorny, I. Fishbein, S. Forbes, I. Alferiev, *IUBMB Life*, 2011, **63**, 613 620.
4. M. Chorny, I. Fishbein, B. B. Yellen, I. S. Alferiev, M. Bakay, S. Ganta, R. Adamo, M. Amiji, G. Friedman, R. J. Levya, *Proc. Natl. Acad. Sci. USA*, 2010, **107**, 8346 8351.
5. V. Farooq, B. D. Gogas, P. W. Serruys, *Cardiovasc. Interv.*, 2011, **4**, 195 205.
6. G. McDowell, M. Slevin, J. Krupinski, *Vasc. Cell*, 2011, **3**, 1 8.
7. S. Prijic, G. Sersa, *Radiol Oncol.*, 2011, **45**, 1 16.
8. O. Vittorio, V. Voliani, P. Faraci, B. Karmakar, F. Iemma,S. Hampel, M. Kavallaris, G. Cirillo, *J. Drug. Target.*, 2014, **22**, 408 415.
9. R. Moreno, C. Macaya, *Curr. Med. Chem. Cardiovasc. Hematol. Agents*, 2005, **3**, 221 229.
10. Y. Huang, L. Wang, I. Verweire, B. Qiang, X. Liu, E. Verbeken, E. Schacht, I. De Scheerder, *J. Invasive Cardiol.*, 2002, **14**, 505 513.

11. K. Larsen, C. Cheng, D. Tempel, S. Parker, S. Yazdani, W. K. den Dekker, J. H. Houtgraaf, R. de Jong, S. Swager-ten Hoor, E. Ligtenberg, S. R. Hanson, S. Rowland, F. Kolodgie, P. W. Serruys, R. Virmani, H.J. Duckers, *Eur. Heart J.*, 2011, **33**, 120 128.
12. D. Tanous, J.H. Bräsen, K. Choy, B.J. Wu, K. Kathir, A. Lau, D.S. Celermajer, R. Stocker, *Atherosclerosis*, 2006, **189**, 342 349.
13. T. Inoue, K. Croce, T. Morooka, M. Sakuma, K. Node, D. I. Simon, *JACC Cardiovasc. Interv.*, 2011, **4**, 1057 1066.
14. H. Hlawaty, M. P. Jacob, L. Louedec, D. Letourneur, C. Brink, J. B. Michel, L. Feldman, M. Bäck, *Arterioscler. Thromb. Vasc. Biol.*, 2009, **29**, 518 524.
15. Y. Kaetsu, Y. Yamamoto, S. Sugihara, T. Matsuura, G. Igawa, K. Matsubara, O. Igawa,C. Shigemasa, I. Hisatome, *Cardiovasc. Res.*, 2007, **76**, 160 166.
16. B. Magnus, *Cardiovasc. Drugs Ther*., 2009, **21**, 41 48.
17. P. Heider, M. Georg Wildgruber, W. Weiss, H. J. Berger, E. H. Henning, O. Wolf, J. *Vasc. Surg.*, 2006, **43**, 969 977.
18. S. Blankenberg, S. Barbaux, L. Tiret, *Atherosclerosis*, 2003, **170**, 191 203.
19. K. Ley, Y. Huo, *J. Clin. Invest*., 2001, **107**, 1209 1210.
20. N. R. Hadi, B. I. Mohammad, A. Almudhafer, N. Yousif, A. M. Sultan, *J. Clin. Exp. Cardiolog.*, 2013, **4**, 1 6.
21. A. J. Robinson, D. Kashanin, F. O'Dowd, V. Williams, G. M. Walsh, *J. Leukoc. Biol*.,2008, **83**, 1522 1529.
22. B. C. Heng, P. P. Bezerra, Q. R. Meng, D. W. Chin, L. B. Koh, H. Li, H. Zhang, P. R. Preiser, F. Y. Boey,S. S. Venkatraman, *Biointerphases*, 2010, DOI: 10.1116/1.3483218.
23. P. K. Thalla, H. Fadlallah, B. Liberelle, P. Lequoy, G. De Crescenzo, Y. Merhi, S. Lerouge, *Biomacromol.*, 2014, **15**, 2512 2520.
24. M. Wen, Q. Li, Y. Li, *J. Electrin Spectros. Relat. Phenom.*, 2006, **153**, 65 70.
25. R. R. Shahraki, M. Ebrahimi, S. A. S. Ebrahimi, S. M. Masoudpanah, *J. Magn. Magn. Mater.*, 2012, **324**, 3762 3765.
26. P. Kinnari, R. V. Upadhyay, R. V. Metha, *J. Magn. Magn. Mater.*, 2002, **252**, 35 38.
27. S. Ammar, N. Jouini , F. Fievet, Z. Beji , L. Smiri, P. Moline, M. Danot, J. M. Greneche , *J. Phys. Condens. Mat.*, 2006, **8**, 9055 9069.
28. L. P. Ol'khovik, Z. I. Sizova, N. V. Tkachenko, V. O. Shein, P. S. Kalinin, E. N. Khats'ko, E. Ya. Levitin, A. A. Koval', *Low Temp. Phys.*, 2010, **36**, 226 229.
29. M. Faraji, Y. Yamini, M. Rezaee, *J. Iran. Chem. Soc.*, 2010, **7**, 1 37.
30. M. A. Willard, L. K. Kurihara, E. E. Carpenter, S. Calvin, V. G. Harris, *Int. Mater. Rev.*, 2004, **49**, 125 170.
31. W. Wu, Q. He, C. Jiang, *Nanoscale Res. Lett.*, 2008, **3**, 397 415.
32. S. Nigama, K.C. Barickb, D. Bahadurb, *J. Magn. Magn. Mater.*, 2011, **323**, 237 243.
33. C. M. Lee, S. Lim, G. Y. Kim, D. W. Kim, J. H. Rhee, K. Y. Lee, *Biotechnol. Lett.*, 2005, **27**, 1487 1490.
34. L. Zhu, J. Ma, N. Jia, Y. Zhao, H. Shen, *Coll Surf., B*, 2009, **68**, 1 6.
35. J. Varshosaz, A. Jafarian Dehkordi, S. Setayesh, *IET Nanobiotechnol.*, submitted.
36. J. Varshosaz, H. Sadeghi Aliabadi, F. Rabbani Khoraskani, *Soft Mater.*, submitted.
37. T. Seternes, I. Oynebråten, K. Sorensen, B. Smedsrod, *J. Exp. Biol.*, 2001, **204**,1537 1546.
38. DC. West, Vascular Endothelium: Physiological Basis of Clinical Problems II, Springer, New York, 1993, 209 210.

39. R. Pigott, L.P. Dillon, I.H. Hemingway, A.J.H. Gearing, *Biochem. Biophys. Res. Commun.*, 1992, **187**, 584 589.

Zinc substituted magnetic nanoparticles (MNPs) were prepared and encapsulated along with sodium montelukast within rosin gum nanoparticles (NPs) by solvent evaporation method. The resulted NPs were targeted to endothelium cells by applying an outer layer of chondroitin sulfate on the surface of NPs. Targeted rosin NPs showed more adhesion to endothelial cells than non-targeted ones and montelukast loaded NPs were more efficient than free drug in suppression of VCAM-1 expression.

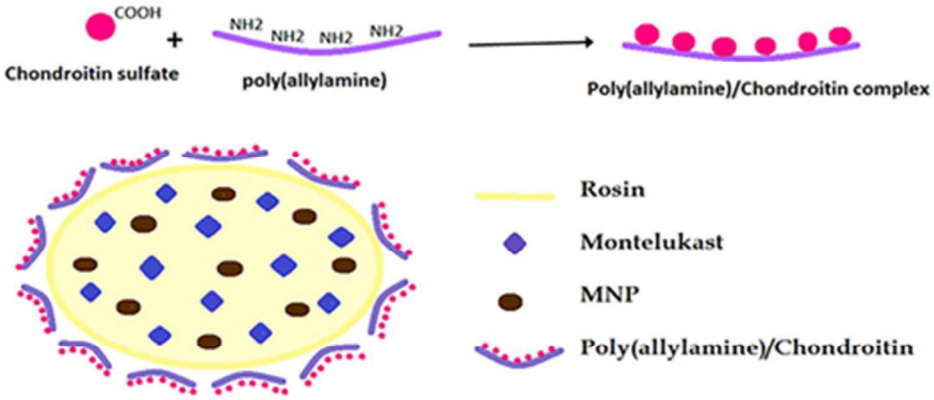

39x19mm (300 x 300 DPI)